Analysis of PV Array coupled Active Network Converter Employing Fuzzy Logic Based Maximum Power Point Tracking Control Strategies

S. EDWARD RAJAN[1], R.PON VENGATESH [2]

[1]Professor, [2] Assistant Professor(Senior Grade), Department of Electrical and Electronics Engineering,

Mepco Schlenk Engineering College, Sivakasi, 626005, Tamil Nadu, India.

Email: sedward@mepcoeng.ac.in, vengateshme@mepcoeng.ac.in

Abstract *- This paper investigates the performance analysis of coupled inductor Active Network Converter (ANC) for photovoltaic (PV) energy harvesting system. The proposed converter has an integrated with two coupled inductors in a single magnetic core which reduces the size of magnetic components and provides high step-up Voltage gain (G_v) without requiring an extreme Duty ratio (D). The voltage conversion ratio of ANC is high and has low switching losses due to the low voltage and current stress of power switches. The Voltage gain characteristic curve of this converter circuit with different turn's ratio (n) has been studied for various duty cycle. The efficiency of this converter is about to 98.73%. Further, this proposed converter is integrated with the PV panel for the harvesting of solar energy. The performance of the solar system for extracting the maximum power depends on the solar irradiance (G), cell temperature (T) and the operating point of Maximum Power Point(MPP) with respect to working conditions. Here, the Incremental Conductance (I&C) algorithm and Fuzzy Logic Control (FLC) method are incorporated for finding the MPP under different operating conditions. The Incremental conductance method overcomes the drawbacks of conventional P&O algorithm. The simulation works have been studied under Matlab-Simulink environment. The effectiveness of the FLC technique adopted in this work for finding MPP has been evaluated and the simulation results are compared with IC method. The simulation results show that the FLC method gives a better improvement in the tracking of MPP than I&C method.*

Key words *- Photo Voltaic (PV), Active Network Converter(ANC), Maximum Power Point Tracking (MPPT), Global Maximum Power Point (GMPP), Incremental Conductance(I&C), PV Module, Fuzzy Logic Control(FLC)*

1. INTRODUCTON

Solar energy is one of the abundantly available energy sources and it is non-polluting the environment and helps in decreasing the greenhouse effect. The nonlinear I–V characteristics of a PV system is a major challenge in PV generation and which has multiple peak power points in its P-V characteristic curve. Hence finding the location of Global Maximum Power Point (GMPP) is the key role for improving the PV system performance. The Incremental Conductance (I&C) algorithm and Fuzzy Logic Control (FLC) method are incorporated for finding the MPP under different operating conditions. The comprehensive PV modeling and simulation of PV arrays are explained in [1-4] various literature works. The Fig.1 shows the Block diagram of the proposed system.

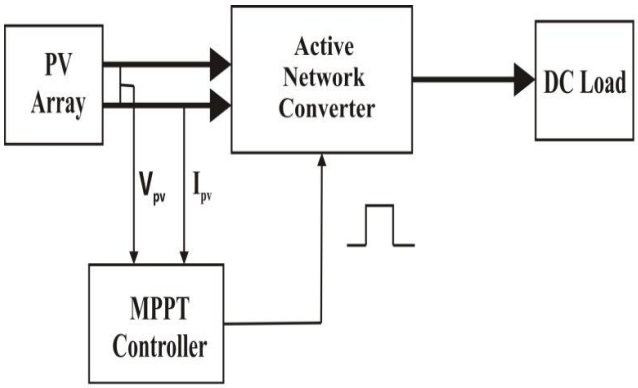

Fig.1. Block diagram of the proposed system

Since, the PV panel has very low conversion efficiency and the proposed integrated coupled inductor Active Network Converter topology transmits solar power from the PV array to the load with high step-up voltage gain without requiring an extreme duty ratio which improves the better efficiency by it minimizing the switching losses.

2. MODELING AND SIMULATION OF ACTIVE NETWORK CONVERTER

High step-up DC–DC power conversion has become one of the important technologies in the modern renewable energy fields. Active Network Converter is a DC-DC converter which increases a low voltage level to a relatively high voltage. As a matter of fact, when the output voltage is high, it is important to reduce the voltage stress on the active switch and output diode; otherwise, it will cause high conduction loss and switching loss. By connecting the coupled inductor to the active network converter, voltage gain can be increased. Furthermore this is explained in [5-10]. Active Network Converter consists of two switches

which can MOSFET, two coupled inductors which can be integrated into one magnetic core, six diodes, one clamping capacitor, and one capacitor as filter in the output side. The Fig. 2 shows the circuit diagram of proposed coupled inductor Active Network Converter.

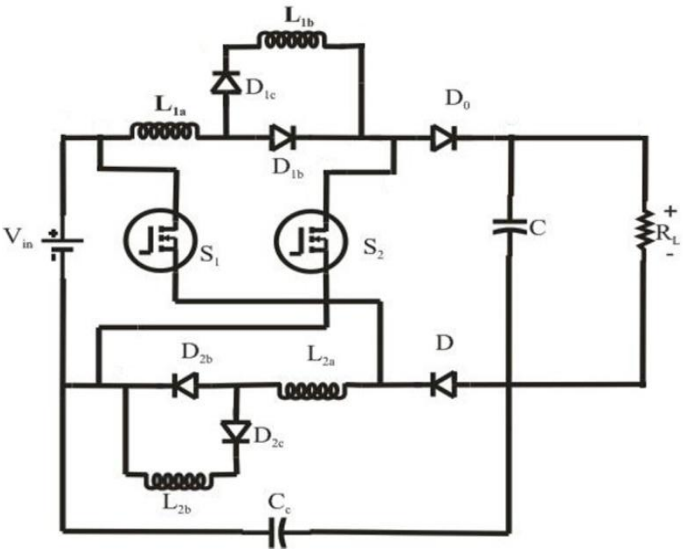

Fig.2. Circuit diagram of proposed coupled inductor Active Network Converter

2.1. Modes of operation of ANC Converter

The performance of converter circuits has been explained in four operating modes as below:

Mode-I operation: During Mode-I the power MOSFET switches of S_1, S_2 are turned ON. The current through the diodes of D_{1c} and D_{2c} decrease to zero at the time of t_0. The inductors of L_{1a} and L_{2a} are charged by the source current and the filter capacitor C releases energy to the load.

Mode-II operation: At the time of t_1, the power switches of S_1 and S_2 are turned OFF; the diodes of D_{o1}, D_{o2}, D_{1c}, and D_{2c} start to conduct. Affected by the leakage inductor, the currents through the inductors of iL_{1a} and iL_{2a} is limited; and as a result of L_{k1} larger than L_{k2}, iL_{1a} decrease slowly than iL_{2a} , the current iC_c could be expressed as $iC_c = iL_{2a-1a} < 0$, clamp capacitor C_c has been discharged. Since $iL_{1a} - iL_{1b} > 0$, $iL_{2a} - iL_{2b} > 0$, D_{1b} and D_{2b} remain conducting during this stage.

Mode-III operation: During this stage, the switches of S_1, S_2 are in OFF state. At the time of t_2, the current through D_{1c} and D_{2c} decrease to zero; the inductors can supply the energy to the load. Since the difference of the leakage inductors, iL_{1b} larger than iL_{2b}, clamp capacitor C_c has been charged.

Mode-IV operation: The switches of S_1 & S_2 start to conduct at the time of t_3; the output diode D_o become reverse-biased; the inductor current iL_{1a} and iL_{2a} increase slowly; the current in the inductors of iL_{1b} and iL_{2b} decrease slowly. The diodes of D_{1c} and D_{2c} keep conducting during this time period.

2.2. Performance analysis of converter

During the ON-state, the inductors of L_{1a} , L_{1b}, L_{2a}, L_{2b} are charged by the dc source, respectively, while, during the OFF State, the inductors are discharged in series.

The derived voltage gain is expressed as,

$$G_V = \frac{1+2D}{1-D} \quad \ldots (1)$$

D is the duty ratio of switches S_1 and S_2. Obviously, we can conclude that all the inductors are sharing the same operation modes, therefore, L_{1a}, L_{1b}, L_{2a} and L_{2b} can be integrated into one magnetic core, as shown in Fig.4. In this condition, we can change the turns ratio of L_{1a}:L_{1b} to 1:n ($n > 1$). When the switches are ON, L_{1a} and L_{2a} are charged by the dc source through D_{1b} and D_{2b}. Since the voltage of L_{1b} and L_{2b} is higher than L_{1a} and L_{2a}, D_{1a} and D_{2a} are reverse biased, When the switches are OFF, L_{1a}, L_{1b}, L_{2a} and L_{2b} are series connected to transfer the energy to output. Due to the circuit symmetry of the proposed converter, it is reasonable to consider $L_{1a} = L_{2a} = L_a$, $L_{1b} = L_{2b} = L_b$, and the turns ratio of two coupled inductors are equaled to *1: n*, the performance analysis of the circuit is illustrated as follows:

2.2.1 Voltage-Conversion Ratio

In an ideal condition, the leakage inductance is zero; the operating mode can be simplified to Mode-I and Mode-III.

During the Mode-I, the voltage across the inductors can be expressed as equation (2.1) & (2.2)

$$V_{L1a} = V_{L2a} = V_i \quad \ldots (2.1)$$

$$V_{L1b} = V_{L2b} = nV \quad \ldots (2.2)$$

During the Mode-III, the voltage across the inductor is expressed as equation (3.1, 3.2 & 3.3),

$$V_{L1a} = V_{L2a} = \frac{V_i - V_o}{2(n+1)} \quad \ldots (3.1)$$

$$V_{L1b} = V_{L2b} = \frac{n(V_i - V_o)}{2(n+1)} \quad \ldots (3.2)$$

$$V_{Cc} = \frac{(V_o - V_i)}{2} \quad \ldots (3.3)$$

By simplifying (3.3), the voltage of clamp capacitor Cc is expressed by equation (4)

$$V_{Cc} = V_o \frac{(n+1)D}{1+(2n+1)D} \quad \ldots (4)$$

By varying the duty cycle (D), Voltage gain of the converter is also varied. According to the turn's ratio,

higher the value of turns gain, the voltage becomes too high (Fig.3). The voltage conversion ratio can be extended by increase *n*.

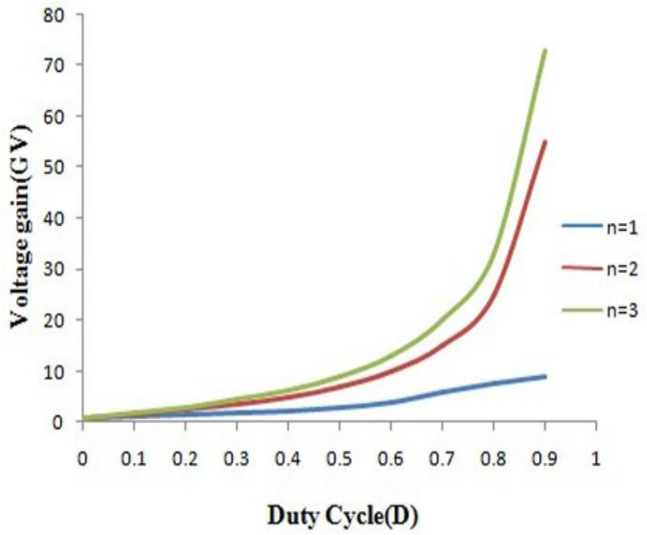

Fig.3. Voltage gain characteristics curve of ANC converter for different turn ratio (n).

The voltage-conversion ratio of the proposed CL-ANC is

$$G_{CCM}=\frac{Vo}{Vi}=\frac{1+(2n+1)D}{1-D} \quad \ldots (5)$$

2.2.2 Effect of Leakage Inductance on Voltage Gain

According to the analysis, the leakage inductor may cause duty-cycle loss and reduce the voltage conversion ratio. Taking the leakage inductor into consideration, the voltage gain is derived as below:

$$G'_{CCM}=\frac{V_o}{V_i}=\frac{\frac{1+(2n+1)D}{1-D}+\sqrt{[\frac{1+(2n+1)D}{1-D}]^2-\frac{8n^2L_kF_sP_o}{[1-D]^2Vi^2}}}{2} \quad \ldots(6)$$

2.2.3 Voltage and Current Stress of the Power Devices

The voltage stress of the diode D_{1c} and D_{2c} can be expressed as below:

$$V_{stress}-D_{1c}=V_{stress}-D_{2c}=nV_i \quad \ldots (7)$$

The voltage stress of the diode D_{1b} and D_{2b} can be expressed as below:

$$V_{stress}-D_{1b}=V_{stress}-D_{2b}=\frac{n(V_o-V_i)}{2(n+1)} \quad \ldots (8)$$

The on-state average current of D_{1c}, D_{2c} can be expressed as equation (9),

$$I_2=\frac{I_o}{1-D} \quad \ldots (9)$$

According to the flux balance on the coupled inductor, the primary current and turns can be expressed by equation (10),

$$N_1I_1=(N_1+N_2)I_2 \quad \ldots (10)$$

Where N_1, N_2 is the number of turns of L_a, L_b, which can be expressed by equation (11),

$$N_2=nN_1 \quad \ldots (11)$$

From (7) & (8) the on-state average current of D_{1b}, D_{2b} can be expressed as equation (12),

$$I_1=\frac{(1+n)I_o}{1-D} \quad \ldots (12)$$

The RMS current through the switches can be obtained be obtained by assuming the inductor current ripple of D_{1b}, D_{2b} which can be expressed by equation (13)

$$\Delta i_L=K_iI_L \quad \ldots (13)$$

$$I_{RMS}=\sqrt{\frac{1}{T_s}\int_0^{DT_s}(I_L-\frac{1}{2}\Delta i_L+\frac{\Delta i_L}{DT_s})^2dt} \quad \ldots (14)$$

$$=\frac{(1+n)\sqrt{D}}{1-D}\frac{P_o}{V_o}\sqrt{(\frac{1}{12}-Ki^2+1)} \quad \ldots (15)$$

The proposed Active Network Converter is simulated in Matlab-Simulink environment with the design specifications for (n=1:1) as mentioned in Table-I.

TABLE –I DESIGN SPECIFICATIONS OF ACTIVE NETWORK CONVERTER

Parameter	Value
Input voltage (V_{in})	21 V
Output voltage (V_{out})	200V
Output power(P_{out})	200W
Switching frequency(fs)	50kHZ
Coupled inductors(L_1,L_2)	330 µ H
Clamping capacitor(Cc)	3 µ F
Capacitor	1 µ F

Fig. 4 shows the Matlab-Simulink diagram of Active Network Converter. Fig. 5 depicts the simulation response of Input-Output waveforms of Active network Converter.

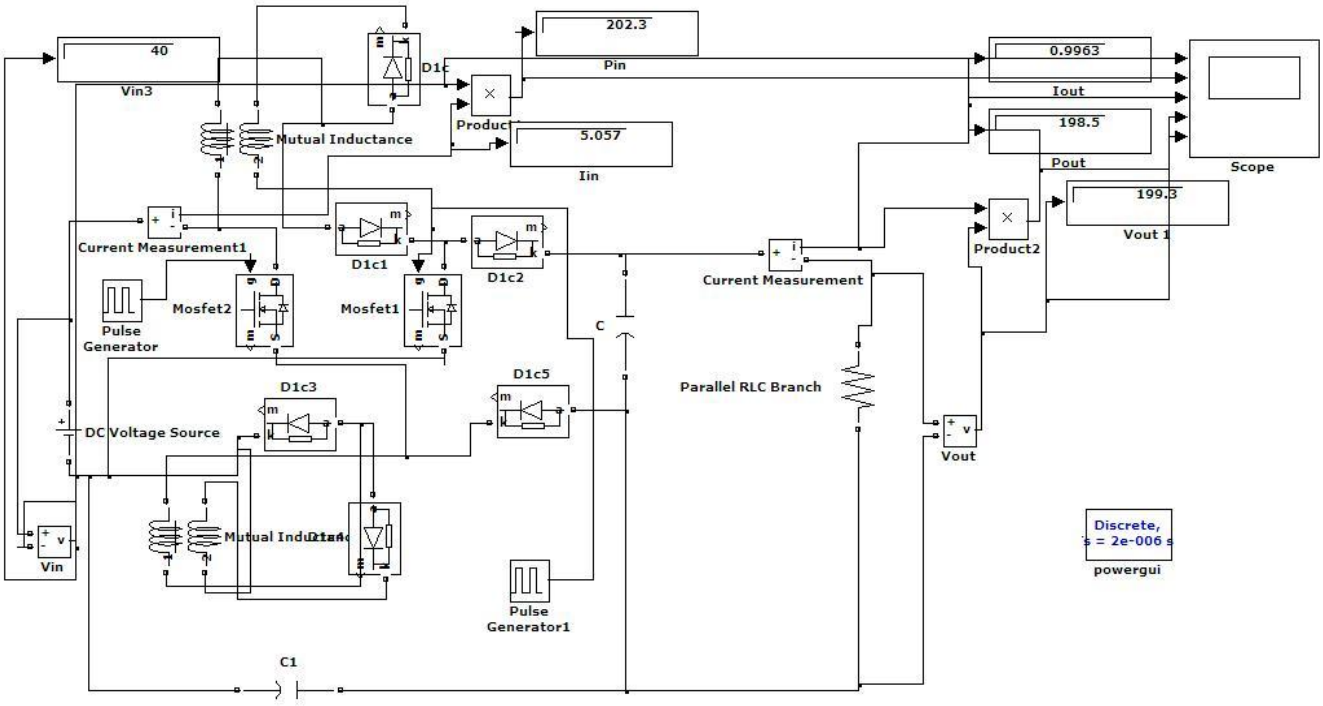

Fig.4. Matlab-Simulink model of proposed Active Network Converter

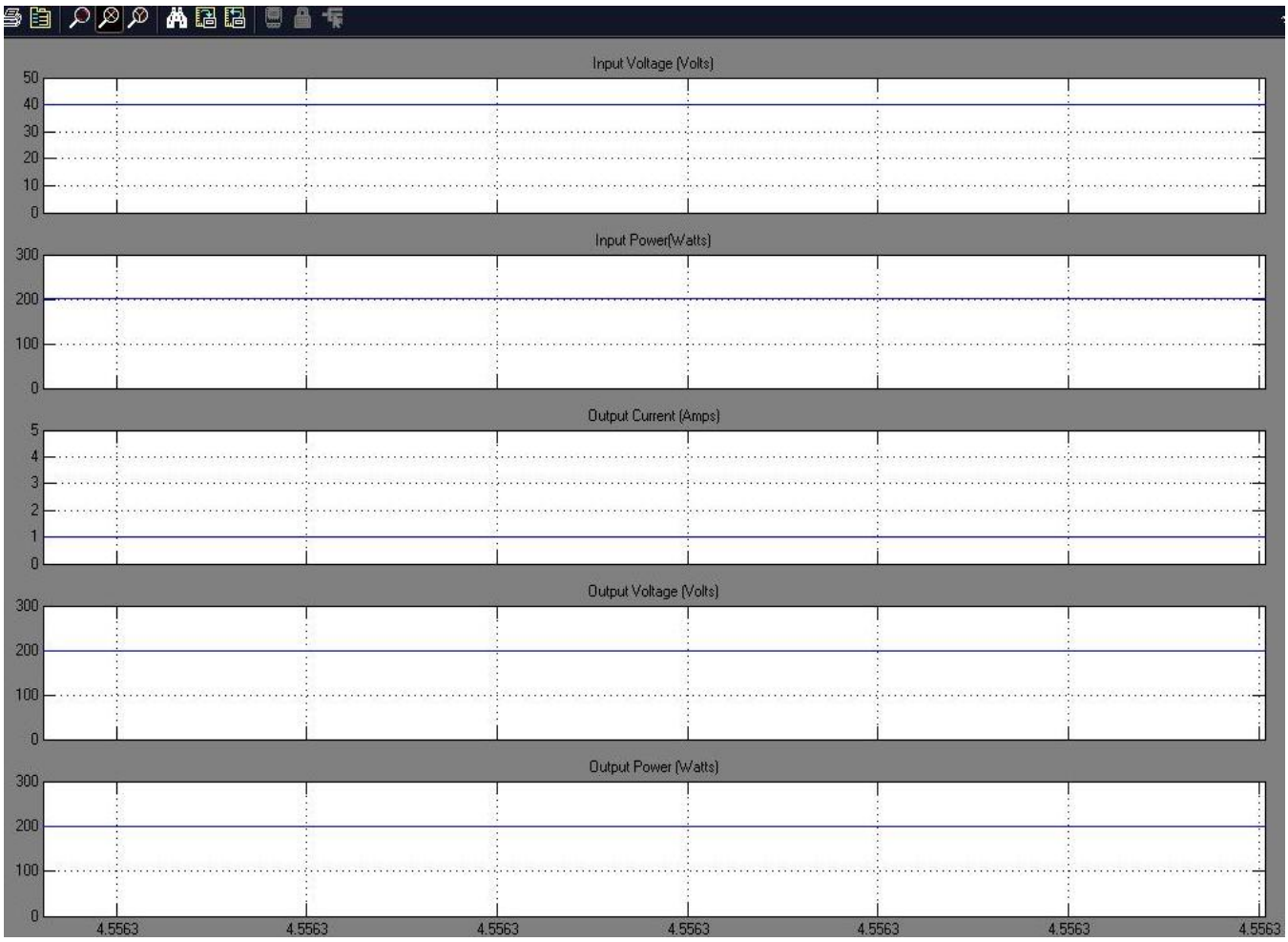

Fig.5. Simulation response of Input-Output waveforms of Active Network Converter

TABLE-II
ANALYSIS OF PROPOSED ACTIVE NETWORK CONVERTER

V_{in} (V)	I_{in} (A)	P_{in} (W)	V_{out} (V)	I_{out} (A)	P_{out} (W)	Efficiency η (%)
20	9.9	197.5	195.5	0.992	194.1	98.23
30	6.6	198.2	196.6	0.993	195.4	98.59
40	5.1	202.5	199.5	1	199.5	98.73

Table-II shows the analysis of proposed converter for the changes in input voltage levels. The proposed converter is analyzed with the different input voltage. As the output voltage of the converter increases the output power also increases. The power output from the proposed converter with input DC source is nearly 200W.

3. MODELING AND SIMULATION OF PV ARRAY

The comprehensive PV module has been developed and simulated in Matlab-Simulink environment. The PV module (MS24250) used in this research work has been referred from manufacturer PV module datasheet. The I-V and P-V characteristics curve of a PV module for different irradiances (1000W/m^2, 800W/m^2 & 600W/m^2) and temperature of 25°C & 30°C have been simulated and plotted in Fig.6 and Fig.7 respectively. The change in irradiation significantly affects the photovoltaic current and change in temperature significantly affects the open circuit voltage and results in the performance of the PV system & Maximum Power Point gets affected [11].

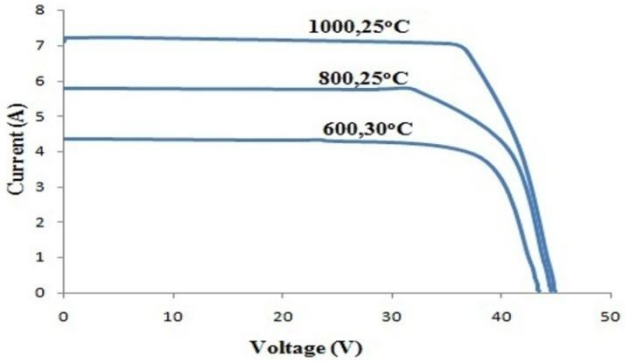

Fig.6.V-I characteristics of a PV module

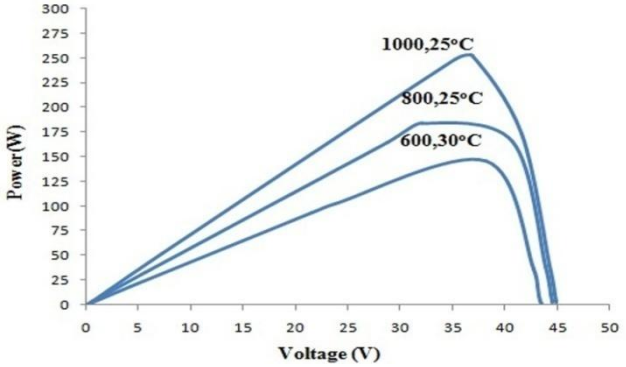

Fig.7.P-V characteristics of a PV module

3.1 MPPT- Incremental Conductance (I&C) algorithm

The IC MPPT method purpose is to find and adjust the array operating voltage by maintaining MPP condition through simple incremental conductance and instantaneous conductance measurement. P&O and IC MPPT controllers are one of the well-known methods which have been employed along this proposed boost converter for comparisons [12]. The Incremental Conductance algorithm (Fig.8) computes Maximum Power Point by comparison of the conductance (dI/dV) to the panel conductance (I/V) when these two are the same (I/V = dI/dV) the output voltage is the MPP voltage is to the right side curve of the MPP and positive when it is to the left side curve of the MPP.

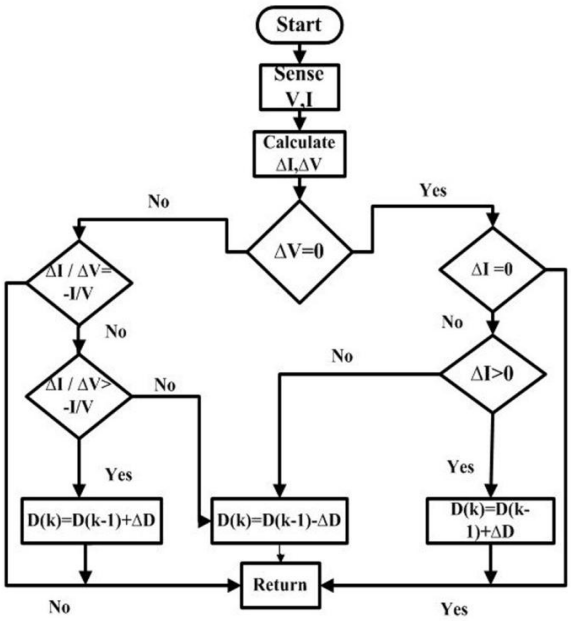

Fig.8.Flowchart for I&C algorithm

This algorithm has advantages over P&O in that it can determine when the MPPT has reached the MPP, where P&O oscillates around the MPP. Also, incremental conductance can track rapidly increasing and decreasing temperature or irradiance conditions with higher precision than Perturb & Observe. The output voltage and current tapped from PV module are given to the MPPT controller and the controller provides an appropriate pulse signal to the power switches in the converter circuit in order to adjust the turn-ON and turn-OFF periods.

3.2 Fuzzy Logic Control (FLC) algorithm

Fuzzy logic based MPPT control technique has been incorporated with ANC converter to study the performance of the PV system. It is relatively simple to design since they do not require the awareness of the exact model. Moreover, it overcomes the conventional MPPT methods of solar power extraction with nonlinearity behavior of the solar

system. The important points should keep in the mind while framing the Rule base of the fuzzy controller [13, 14].

The error (E) and change in error (CE) are the two FLC input variables and the respective duty ratio (D) is referred as fuzzy output. The fuzzy membership values are referred as NB-Negative Big, NS-Negative Small, ZE-Zero, PS-Positive Small and PB-Positive Big. The mathematical expression for Error (E) and Change in Error (CE) are as shown in equation (16) & equation (17). The Triangular membership functions are used here and are plotted in Fig.9& Fig.10.

$$E(j) = \frac{P_{pv}(j) - P_{pv}(j-1)}{V_{pv}(j) - V_{pv}(j-1)} \quad \ldots (16)$$

$$CE(j) = E(j) - E(j-1) \quad \ldots (17)$$

Where P_{pv} (j) and V_{pv} (j) are the instant power and voltage of the photovoltaic module respectively.

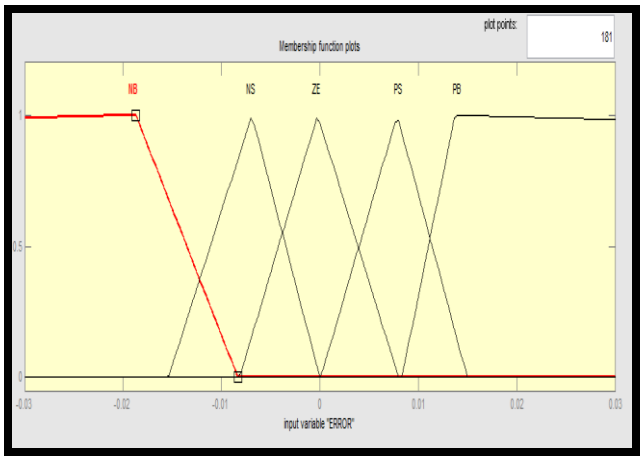

Fig.9.Membership function for error

Where P_{pv}, V_{pv} are the PV power and voltage respectively at instant j. E (j) shows if the load operating point at the Instant j is located on the left or on the right of the maximum power point on the P-v characteristics where it equals to zero at MPP. While the change of error CE (j) expresses the moving direction of this point.

In this work, Mamdani method of Fuzzy inference system is employed because of its significant capability.
The foundation of a fuzzy mapping rule is a fuzzy graph, which describes the relationship between the fuzzy input and the fuzzy output. In this work, the Fuzzy rule base is a set of IF-THEN rules that contain all the information for the controlling the parameter. The Rule base can be developed with expertise knowledge in the field under the work.

The defuzzification uses the center of gravity to compute the output of this FLC, which can be expressed by equation (18),

$$D = \frac{\Sigma_{j=1}^{n} \mu(D_j) - D_j}{\Sigma_{j=1}^{n} \mu} (D_j) \quad \ldots (18)$$

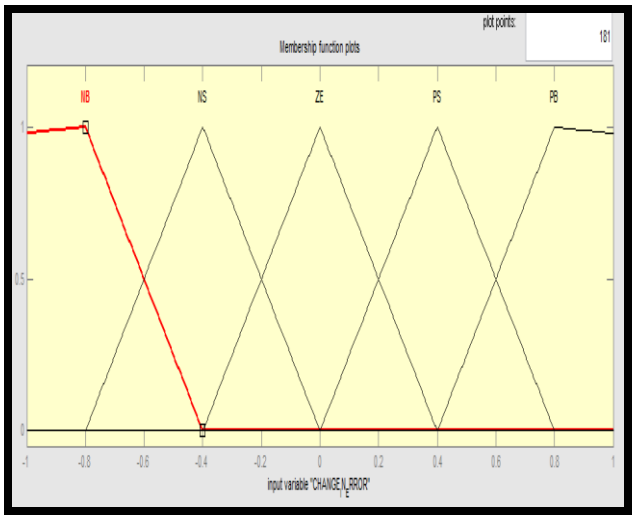

Fig.10.Membership function for change in error

The developed Rule base for this study has been listed in the Table – III. Matlab-Simulink model of a PV module interfaced with the proposed converter under 1000W/m^2 using FLC algorithm is shown in Fig.11 and the Input-Output simulation responses under solar irradiation 800W/m^2 using FLC algorithm is illustrated in Fig. 12.

TABLE-III FUZZY RULE BASE

CE / E	NB	NS	ZE	PS	PB
NB	ZE	ZE	PB	PB	PB
NS	ZE	ZE	PS	PS	PS
ZE	PS	ZE	ZE	ZE	NS
PS	NS	NS	NS	ZE	ZE
PB	NB	NB	NB	ZE	ZE

Comparative analysis of I&C and FLC algorithm under 1000W/m^2, 25˚C, 800W/m^2, 30˚C, 600W/m^2, 25˚C conditions are tabulated in Table-IV and it is inferred that the output power gets improved in Fuzzy control in compared to I&C method.

TABLE-IV -COMPARATIVE ANALYSIS OF I&C AND FLC MPPT ALGORITHM.

Operating conditions	**MPPT**	**V_{out} (V)**	**I_{out} (A)**	**P_{out} (W)**	**H (%)**
1000W/m^2, 25°C	I&C	196	0.97	191	96
	FLC	198	0.98	195	97
800W/m^2, 30°C	I&C	193	0.96	186	94
	FLC	196	0.97	192	96
600W/m^2, 25°C	I&C	190	0.94	180	91
	FLC	195	0.96	188	95

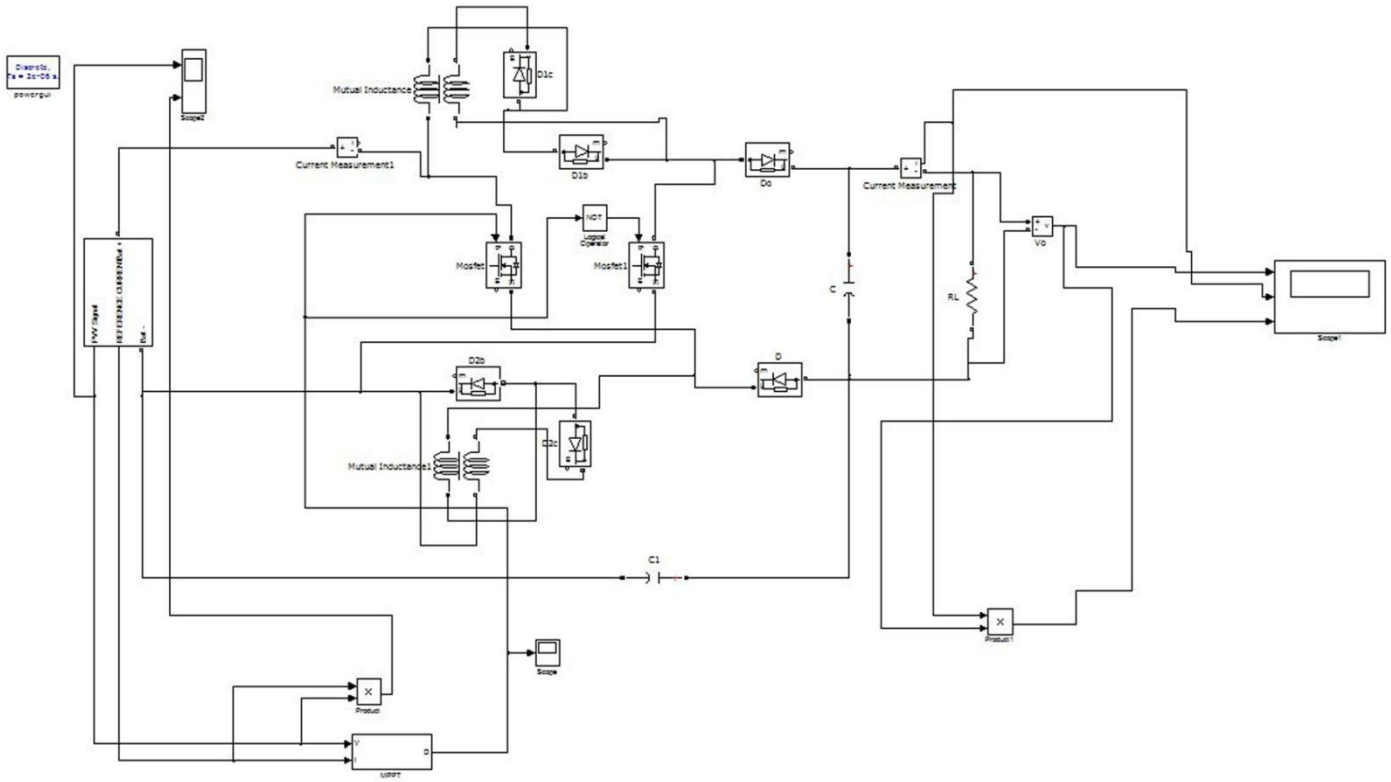

Fig.11.Matlab-Simulink model of a PV-module interfaced with the proposed converter under 1000W/m^{2}with FLC algorithm

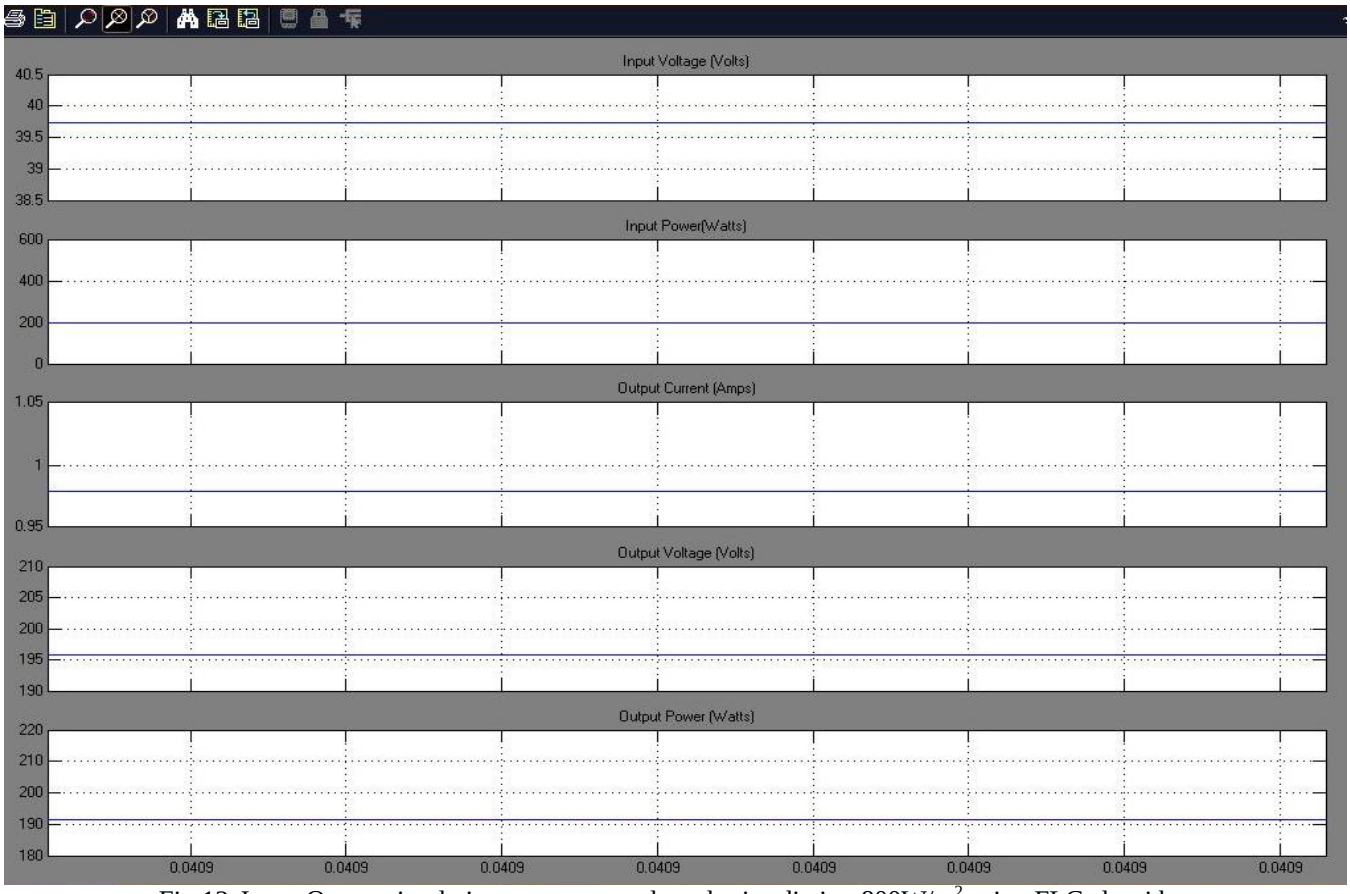

Fig.12. Input-Output simulation responses under solar irradiation 800W/m^2 using FLC algorithm

4. CONCLUSION

This paper investigated the performance analysis of coupled inductor Active Network Converter (ANC) for a standalone photovoltaic energy harvesting system. The Voltage gain characteristic curve of this converter circuit with different turn's ratio (n) has been studied for various duty cycles. The Input-Output responses of the proposed converter for different voltage levels have been analyzed. Further, this proposed converter is integrated with the PV array for the harvesting of solar energy. The modular characteristics of PV module under different irradiance level and temperature have been analyzed using Matlab-Simulink environment. Here, the Incremental Conductance (I&C) algorithm and Fuzzy Logic Control (FLC) method are incorporated for finding the MPP under different operating conditions. The Fuzzy Rule base is also illustrated & the effectiveness of the FLC technique adopted in this work for finding MPP has been evaluated and the simulation results are compared with IC method. The simulation results show that the FLC method gives a better improvement in the tracking of MPP than I&C method. Further, this converter-PV system can be connected with On-grid interactive with suitable power inverter circuits for meeting the power demands.

References

[1] N.Mutoh, M.Ohno, T.Inoue, "A Method for MPPT Control while Searching for Parameters Corresponding to Weather Conditions for PV Generation Systems," *IEEE Transactions on Industrial Electronics, vol. 53, NO. 2, pp. 1055-1065,* 2004.

[2] P. S. Revankar, W. Z. Gandhare and A. G. Thosar Government College of Engineering, Aurangabad, "Maximum Power Point Tracking for PV Systems Using MATLAB/SIMULINK", Second International Conference on Machine Learning and Computing, 2010.

[3] M. G. Villalva, J. R. Gazoli, E. Ruppert F, "Modeling and circuit-based simulation of photovoltaic arrays", *Brazilian Journal of Power Electronics,* ISSN 1414-8862, vol. 14, no., pp. 35-45, 2009.

[4] A. Chitra, S. Rose Mary, Palackal, K.Greeshma, Viswanathan and Nirupama Nambiar,"An Incremental Conductance Based Maximum Power Point Tracking Algorithm for a Solar Photovoltaic System," *International Journal of Applied Engineering Research*, ISSN 0973-4562, Vol. 8, No. 19, 2013 pp. 2299-2302.

[5] K.C.Tseng and C.C.Huang, "High step-up high efficiency interleaved converter with voltage multiplier module for renewable energy system," *IEEE Trans.Ind.Electron., Vol.61, no.3, pp.1311-1319*, Mar-2014.

[6] T.Wang, Y.Tang, and Y.H.He, D.J.Fu, and J.R.Kan, "Study of a coupled inductor converter based active-network," *in Proc. IEEE Ind.Electron.Soc.,2013, pp. 1302-1307.*2.

[7] T.Wang, Y.Tang, and Y.H.He, D.J.Fu, "Study of a high step-up voltage gain DC-DC converter with passive lossless clamp circuit," *in Proc. IEEE Ind.Electron. soc.,2013 pp. 1308-1313*

[8] Y.P.Hsieh, J.F.Chen, L.s.Yang, C.Y.Wu, and W.S.Liu, "Novel high step-up DC-DC converter with coupled-inductor and switched-capacitor techniques," *IEEE trans.Ind.Electron,* vol.59, no. 2, pp. 998-1007, Feb- 2012.

[9] Y. P. Hsieh, J. F. Chen, L. S. Yang, C. Y. Wu, and W. S. Liu, "High conversion- ratio bidirectional dc/dc converter with coupled inductor, "*IEEE Trans. Ind. Electron.*, vol. 61, no.1, pp. 210–222, Jan-2014.

[10] L. S. Yang, T. J. Liang, and J. F. Chen, "Transformerless DC–DC converters with high step-up voltage gain," *IEEE Trans. Ind. Electron,* vol. 56, no. 8, pp. 3144–3152, Aug. 2009.

[11] R. Pon Vengatesh, S. Edward Rajan, "Investigation of the effects of homogeneous and heterogeneous solar irradiations on multi-crystal PV module under various configurations," *IET Renewable Power Generation,* ISSN: 1752-1416,Vol.9, No.3, Page No.:245-254, April 2015.

[12] Amarnath Kurella, R Suresh, "Simulation of Incremental Conductance MPPT with direct control method using Cuk Converter," *IJRET: International Journal of Research in Engineering and Technology,* Vol.2, No.9, pp.557-566, Sep. 2013.

[13] O. Cordon and F.H.M.J. Jesus, "A proposal on reasoning methods in fuzzy rule-based classification systems", *International Journal of Approximate Reasoning,*Vol 20, pp. 21–45. 1999.

[14] CHEN Jun, HUI Jing, "Study on MPPT for Photovoltaic Generation Based on Fuzzy-control Strategy," *Modern Electronic Technology*, vol. 293, pp. 182–185,2009.